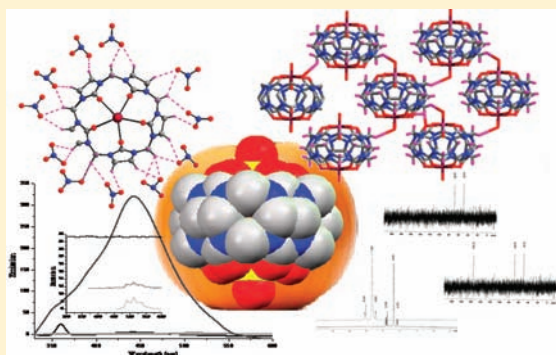


Fluorescent Uranyl Ion Lidded Cucurbit[5]uril Capsule

S. Kushwaha,[†] Srinivas A. Rao,[‡] and Padmaja P. Sudhakar^{*,†}[†]Department of Chemistry, Faculty of Science, The M.S. University of Baroda, Vadodara-390002[‡]School of Chemistry, Hyderabad Central University, Hyderabad-500046

Supporting Information

ABSTRACT: A novel fluorescent complex $\{(UO_2)_2(CB5)\} \cdot (NO_3)_4 \cdot 4HNO_3 \cdot 3H_2O$ (U2CB5) is obtained from cucurbit[5]uril (CB5) and uranyl nitrate under ambient temperature conditions. The crystal structure revealed that two uranyl ions are coordinated to the two open portals of CB5 giving a closed molecular capsule, which further connected through CB5 molecules to give two-dimensional frameworks. The U2CB5 complex was further investigated by NMR, FTIR and TGA techniques. The Fluorescence of uranyl ion was found to be enhanced due to complexation with cucurbituril.

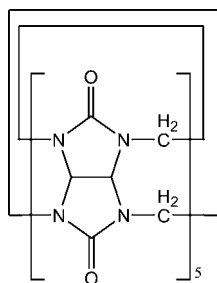


INTRODUCTION

Cucurbiturils are highly symmetrical pumpkin shaped macrocycles with two identical dipolar portal ends composed of carbonyl functional groups that were developed after cyclodextrins, crown ethers and calixarenes.^{1–3} The metal complexing properties of cucurbiturils have been widely investigated,^{4,5} particularly in the case of alkali, alkaline-earth,⁶ lanthanide cations⁷ and d-block metal ions.⁸ In the case of actinides, the crystal structures of only two compounds have been reported by Fedin et al., one having Th(IV) cation bound to three adjacent carbonyl groups complexed at each portal of CB6, and the other $[(UO_2)_4(\mu_3-O)_2(\mu_2-Cl)_4(H_2O)_6]$.⁹ CB6, having no uranium–carbonyl bond, the tetranuclear uranyl complex being only hydrogen bonded to the macrocycle.¹⁰ These molecules exhibit wide range of applications including molecular catalysis, molecular recognition, ion channel, and supramolecular assemblies.¹¹

Recent synthesis of cucurbituril homologues (CB[n], n = 5, 7 and 8) (Scheme 1) has broadened the scope of the cucurbituril

Scheme 1. Cucurbit[5]uril



chemistry.¹² Thuery was the first to report complexes between uranyl ions and CB5, the heterometallic uranyl lanthanide

complexes having direct uranyl-carbonyl bonds and hydrogen bonded channels.¹³ Polynuclear complexes were also reported by him where uranyl ions were bound to two carbonyl groups from two different molecules.¹³ CB5 is known to form capsules when capped by alkali metal⁷ or lanthanide ions, and Zn, K with different cations at its two portals.^{8d,13a,14} In the absence of other reactants (alkali metal/lanthanide ions, Zn and K) the problem of formation of insoluble powders and/or small quantity of crystals was reported by Thuery under hydrothermal conditions.¹³ However during the course of our attempt to prepare a complex of uranyl nitrate with CB5 under ambient conditions we were pleasantly surprised to get yellow crystals of U2CB5 at ambient temperature conditions, in which both the portals are closed by uranyl ions. Since the fluorescent characteristics of uranyl ions is well-known we were curious to investigate the fluorescence behavior of U2CB5.

We thus report herein the synthesis, characterization and single crystal X-ray structure analysis of (U2CB5). The uniqueness of this complex is linkage of two uranyl moieties with CB5 and its fluorescence behavior. Binuclear coordination complexes of uranyl ions with cucurbituril and their fluorescence properties have hitherto not been reported though there have been studies on the effects of encapsulation by cucurbituril on the fluorescence of guest molecules like 1-Anilinonaphthalene-8-sulfonate, rhodamine 6G, curcumin, coumarin, carbendazim, berberine, alkaloids, riboflavin, coptisine, melamine, sanguinarine, pyrene, and tropicamide.^{12,15}

EXPERIMENTAL SECTION

Synthesis of $\{(UO_2)_2(CB5)\} \cdot (NO_3)_4 \cdot 4HNO_3 \cdot 3H_2O$ (U2CB5). $UO_2(NO_3)_2 \cdot 6H_2O$ was purchased from Sulab chemicals, HNO_3 was

Received: July 29, 2011

Published: November 30, 2011

purchased from E-Merck and cucurbit[5]uril from Aldrich. Cucurbit[5]uril (20 mg, 0.020 mmol) was dissolved in 4.6 mL of demineralized water and 0.4 mL of HNO₃ (69% w/v) was added to it. A 10-fold excess of UO₂(NO₃)₂·6H₂O (116 mg, 0.232 mmol) was dissolved in 4.9 mL of demineralized water and 0.1 mL of HNO₃ (69% w/v) was added to it. The uranyl nitrate solution was added dropwise to cucurbituril solution with continuous stirring and was left for 24 h at 40 °C under stirring conditions and the complex is readily synthesized. Light yellow color crystals of the complex U2CB5 were deposited in solution. Good quality single crystals of light yellow color could be separated within 24 h, which if left further for another 24 h resulted in crystalline material (Supporting Information Figure S1). Anal. Calcd. for C₃₀H₄₀N₂₈O₄₁U₂: C, 18.75; H, 2.08; N, 20.42. Found C, 18.82; H, 1.97; N, 20.54%. The observed percentage of U was found to be 12.41% (Anal. Calcd. 12.39%). ¹H NMR (D₂O/HCl 300K): δ (ppm) 6.873, 8.190 (d, -CH₂-) and 8.073 (s, -CH-) for U2CB5. ¹³C NMR (D₂O/HCl 300K): δ (ppm) 51.13, 71.78, and 172.88 for U2CB5.

Crystallographic Studies. A yellow single crystal of suitable size and uniform shape was selected and mounted on a glass fiber with epoxy and aligned on a Bruker SMART APEX CCD X-ray diffractometer. Intensity measurements were performed using graphite monochromated Mo K_α radiation [$\lambda = 0.71073$ Å]. Each set had a different Φ angle for the crystal, and each exposure covered a range of 0.3° in ω . A total of 2400 frames were collected with an exposure time per frame of 40 s. ω scan width of 0.3°, each for 8 s, crystal-detector distance 60 mm, collimator 0.5 mm. The data were reduced by using SAINTPLUS and a multiscan absorption correction was done using SADABS.¹⁶ Structure solution and refinement were performed using SHELX-97.¹⁶ All non hydrogen atoms were refined anisotropically. The final cell parameters were determined using a least-squares fit to 4713 reflections. During the crystallography 25040 reflections were collected, among which 4713 unique ones were used to solve the structure with $R(\text{int}) = 0.0343$. Crystallographic data for the structure reported in this paper have been deposited with the Cambridge Crystallographic Data Centre as supplementary publication no. CCDC-826208. Copies of the data can be obtained free of charge on application to CCDC, 12 Union Road, Cambridge CB21EZ, UK (fax: (0.44) 1223-336-033; e-mail: deposit@ccdc.cam.ac.uk).

¹H and ¹³C NMR Spectroscopy. High-resolution ¹H and ¹³C NMR spectra were recorded using a Varian-500 spectrometer operating at 500 MHz in D₂O/HCl. The chemical shifts δ , expressed in parts per million [ppm], were referenced relative to the signal of tetramethylsilane (Si(CH₃)₄) at $\delta = 0$ ppm.

Fluorescence Spectroscopy. Fluorescence and absorption data were acquired for the solutions of ligand and the compound using a Jasco spectrofluorimeter quartz cell and Lamda-35 Perkin-Elmer UV-visible spectrophotometer. Excitation was achieved using 365 nm light from a Xenon lamp for the fluorescence spectroscopy. The absorption spectra are provided in the Supporting Information. Absolute emission quantum yields were determined by comparison of the integrated emission intensity with that of quinine sulfate under identical conditions such as exciting wavelength, optical density, and apparatus parameters.

Powder X-ray Diffraction. Powder X-ray diffraction pattern of the samples were collected on a PHILIPS PW-1830. XRPD pattern of the ingredients was taken by holding in place on quartz plate for exposure to CuK α radiation of wavelength 1.5406 Å. The sample was analyzed at room temperature over a range of 10–70° 2 θ with sampling intervals of 0.02° 2 θ and scanning rate of 2°/min.

Infrared Spectroscopy. Infrared spectra were obtained from single crystals of the compound using a Perkin-Elmer RX1 model FT-IR spectrometer. FT-IR spectra for the crystal was obtained by first mixing with KBr and then ground in a mortar at an appropriate ratio of 1/100 for the preparation of the pellets. The resulting mixture was pressed at 10 tons for 5 min and sixteen scans with 8 cm⁻¹ resolution were applied in recording spectra. The background obtained from the scan of pure KBr was automatically subtracted from the sample spectra. The spectra can be found in the Supporting Information.

Thermal Analysis. The thermal behavior of the crystal was evaluated by using thermo-gravimetric analyzer (TG/DTA 6300

(INCARP EXSTAR 6000), under air at a heating rate of 10 °C min⁻¹ up to 450 °C.

ICP Analysis of Uranium. For the ICP analysis, the U2CB5 complex (5 mg) was dissolved in 10 mL of water. After complete dissolution, the solution was transferred to a 25 mL volumetric flask and diluted to final volume with deionized water. Five standard solutions of uranium were used to obtain calibration curves with concentrations of 1–10 mg L⁻¹ prepared from a 1000 mg L⁻¹ stock solution. The standards and sample were analyzed by an inductively coupled plasma atomic emission spectrophotometer (ICPAES, Thermo Jarrel Ash, Model TraceScan) at wavelengths of 409.014 nm.

Elemental Analysis (EDAX and CHN Analyzer). Elemental analysis was carried out using a JSM5610LV instrument combined with INCA-EDX-SEM analyzer and confirmed by Perkin-Elmer 2400 CHN analyzer for the quantitative identification.

■ RESULT AND DISCUSSION

Synthesis. {(UO₂)₂(CB5)}(NO₃)₄·4HNO₃·3H₂O (U2CB5) can be synthesized under mild room temperature conditions in reasonable yield. Amount of water or dilution and pH of the reaction is an important part playing role for synthesizing U2CB5 as it serves as mineralizing agent as well as counteraction.

Structural Characteristics. The title compound {(UO₂)₂(CB5)}(NO₃)₄·4HNO₃·3H₂O (U2CB5) crystallizes in monoclinic system with space group of C2/c. The asymmetric unit in the crystal structure of U2CB5 is composed of half of the moiety with four units of nitrate anion (two for charge compensation and other two for lattice HNO₃ molecules) and three lattice water molecules. Coordination complexes having two uranyl ions in the same molecular unit to form the internal complex are extremely rare and exhibit interesting properties. But here, in contrast to the reported results we are presenting the first internal complex of uranyl nitrate and cucurbit[5]uril under normal bench conditions.

The full molecule of the U2CB5 as shown in Figure 1 is a biuranyl complex with cucurbit[5]uril (CB5) and crystallo-

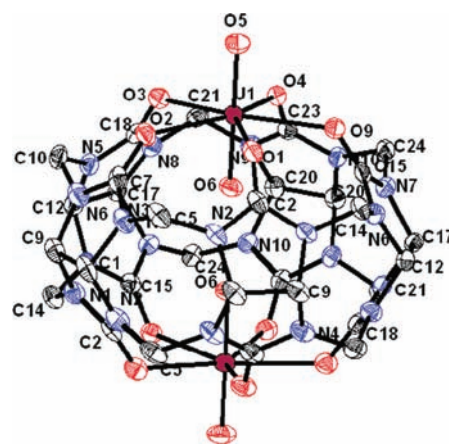


Figure 1. Oak Ridge thermal ellipsoidal diagram of the U2CB5 with 40% probability (Hydrogens, counteranion and solvent water molecules are omitted for clarity): Color code: C, gray; O, red; N, blue.

graphic data with structural refinement parameters are provided in Table 1. Here, uranyl cations fit into both open portals of CB5 molecule. The U–O bond lengths with the five carbonyls of CB5 is in the range of 2.413(4)–2.454(4) Å while in the case of pendant uranyl oxygens it is 1.748(5)–1.759(5) Å. The hydrogen bonding environment around {(UO₂)₂(CB5)}⁴⁺ is

Table 1. Crystallographic Data and Structural Refinement

entry	U2CB5
formula	C ₃₀ H ₃₀ N ₂₈ O ₄₁ U ₂
volume	1914.88
crystal system	monoclinic
space group	C2/c
a/Å	15.0886 (15)
b/Å	14.5869 (14)
c/Å	24.889 (2)
β/deg	93.6340(10)
U/Å ³	5340.6 (9)
Z	4
F(000)	3672
ρ _{cal} / Mg m ⁻³	2.382
crystal size (mm ³)	0.36 × 0.22 × 0.14
completeness to θ = 25.0	100%
θ range for data collection (deg)	1.68–25.0
reflections collected/unique	25040/4713 [R(int) = 0.0343]
R ₁ (F ₀ ²) [I > 2 σ(I)]	0.0349
R ₂ (F ₀ ²) [I > 2 σ(I)]	0.0957
R ₁ (F ₀ ²) (all data)	0.0395
R ₂ (F ₀ ²) (all data)	0.0992
largest diff. peak and hole (Å ⁻³)	1.323 and -1.427

quiet interesting, which is shown in the Supporting Information Figure S2 where the length of C–H...O is 2.40 to 2.80 Å. The hydrogen bonding distances and angles are represented in Table 2. The environment of nitrate anion around {(UO₂)₂(CB5)}⁴⁺ looking like a wheel is shown in Figure 2,

Table 2. Hydrogen Bonds for U2CB5 [Å and deg]^a

D–H...A	d(D–H)	d(H...A)	d(D...A)	∠(DHA)
C(24)–H(24A)...O(2)#2	0.97	2.74	3.460(7)	131.3
C(24)–H(24B)...O(12) #3	0.97	2.39	3.324(8)	162.4
C(20)–H(20A)...O(17)	0.85(6)	2.51(6)	3.275(12)	150(5)
C(21)–H(21B)...O(10) #4	0.97	2.48	3.353(8)	149.4
C(21)–H(21A)...O(15) #5	0.97	2.45	3.297(9)	146
C(17)–H(17)...O(10)#4	0.92(5)	2.47(5)	3.248(9)	142(4)
C(12)–H(12)...O(10)#6	0.87(7)	2.54(7)	3.313(8)	148(5)
C(14)–H(14B)...O(10) #6	0.97	2.81	3.591(9)	138.5
C(14)–H(14A)...O(16) #5	0.97	2.49	3.460(9)	176.6
C(10)–H(10A)...O(7)#7	0.97	2.63	3.429(11)	139.6
C(10)–H(10B)...O(14) #8	0.97	2.89	3.586(10)	129.4
C(10)–H(10B)...O(11) #6	0.97	2.67	3.565(9)	153.2
C(14)–H(14B)...O(11) #6	0.97	2.39	3.331(9)	162.4
C(9)–H(9)...O(13)#9	0.94(7)	2.53(6)	3.226(9)	131(5)
C(5)–H(5B)...O(17)#10	0.97	2.4	3.285(12)	150.7
C(1)–H(1)...O(17)#11	0.89(6)	2.68(6)	3.416(13)	141(5)
C(5)–H(5A)...O(4)#12	0.97	2.47	3.257(7)	138.6

^aSymmetry transformations used to generate equivalent atoms: #1 -x, y, -z + 1/2; #2 -x + 1/2, y + 1/2, -z + 1/2; #3 x - 1, y, z; #4 -x + 1, y, -z + 1/2; #5 x - 1/2, y - 1/2, z; #6 x - 1, -y + 1, z + 1/2; #7 -x + 1/2, -y + 1/2, -z + 1; #8 -x + 1, -y + 1, -z + 1; #9 x - 1, y - 1, z; #10 x, y - 1, z; #11 -x, y - 1, -z + 1/2; #12 -x + 1/2, y - 1/2, -z + 1/2.

C–H...O interaction being responsible for the whole architecture. Extensive O–H...O interaction has been found in the crystal structure of U2CB5, which leads to a 2-dimensional network as represented in Figure 3.

The water molecules are involved in both intra- and intermolecular hydrogen bonding. The distance between the uranium atoms is 6.079 Å, and the separation between the inner oxo groups is 2.562 Å. The water molecules are located in the intermolecular spaces. The uranyl ion is perpendicular to the O plane, with an angle of ~94° with the normal to the plane and the uranium environment is thus a regular pentagonal bipyramid.

The phase purity of U2CB5 was confirmed by XRPD patterns (Supporting Information Figure S1a–c). Peak positions of the experimental and simulated spectra are in good agreement with each other indicating overall homogeneity of the samples and showing that single crystal and bulk properties remains the same. The unit cell parameters from the powder data were found to be in good agreement with that of single crystal. X-ray powder diffraction patterns showed numerous reflections in the low to high angle regions, indicative of crystalline phases. The high intensity Bragg reflections (7.2, 8.7, 12.6, 15.4, 16.9, 18.0, 18.6, 19.9, 20.9, 21.7 Å) are likely due to the strongly scattering uranyl cations.¹⁷

The ¹H decoupled NMR spectrum showed upfield shifting of the signals due to deshielding of protons after complexation. Two doublets (–CH₂–) and a singlet (–CH–) along with a very broad signal (D₂O) appeared at ~4.2 and 5.6 (d), ~5.4 (s) and ~4.7 ppm for CB5 which shifted upfield to ~6.9 and 8.2 (d), 8.1 (s), and 7.3 ppm, respectively, after complexation with uranium (Figure 4). The ¹³C NMR spectrum (Figure 4) showed chemical shifts at 49.91, 68.95, and 156.23 ppm, which can be attributed to N–CH₂–N, N–CH–N, and –C=O groups, respectively, in CB5. While there were small changes in chemical shifts attributed to N–CH₂–N and N–CH–N in U2CB5, the chemical shift of –C=O at 156.23 ppm shifted downfield to 172.88 ppm. This probably indicates the formation of covalent bond between highly electronegative uranyl ion to the carbonyl moiety of CB5.

The DTA curve of CB5 (Supporting Information Table S1 and Figure S3) shows an endothermic transition in the temperature interval 67.704–151.24 °C, which corresponds to a mass loss of 9.13% in the TG curve. This weight loss corresponds to the loss of 4.6 lattice water molecules. CB5 loses most of its weight (52%) around 400 °C. After complexing, DTA curve of U2CB5 showed an endothermic transition in the temperature interval 85.051–172.243 °C. This corresponds to a mass loss of 5.094% in the TG curve equivalent to 5.6 lattice water molecules. An exothermic transition in the temperature interval 270.619–355.758 °C, corresponding to a mass loss of 16.183% in the TG curve occurs due to decomposition of ligand and formation of UO₃.¹⁸ Thus the weight loss is less in U2CB5 around 400 °C in contrast to CB5, but it overlaps with the ligand decomposition and gives a continuous weight loss until the final product UO₃ is formed at about 450 °C.

The selected vibrations from FT-IR spectra of CB5 and U2CB5 with the suggested assignments, are listed in Supporting Information Table S4. The very strong and broad bands found at ~3439 and 3423 cm⁻¹ and sharp bands at 1636 cm⁻¹ in the spectra are consistent with the presence of water molecules in the ligand and complex, also supported by the single crystal XRD. Frequencies of the stretching and bending

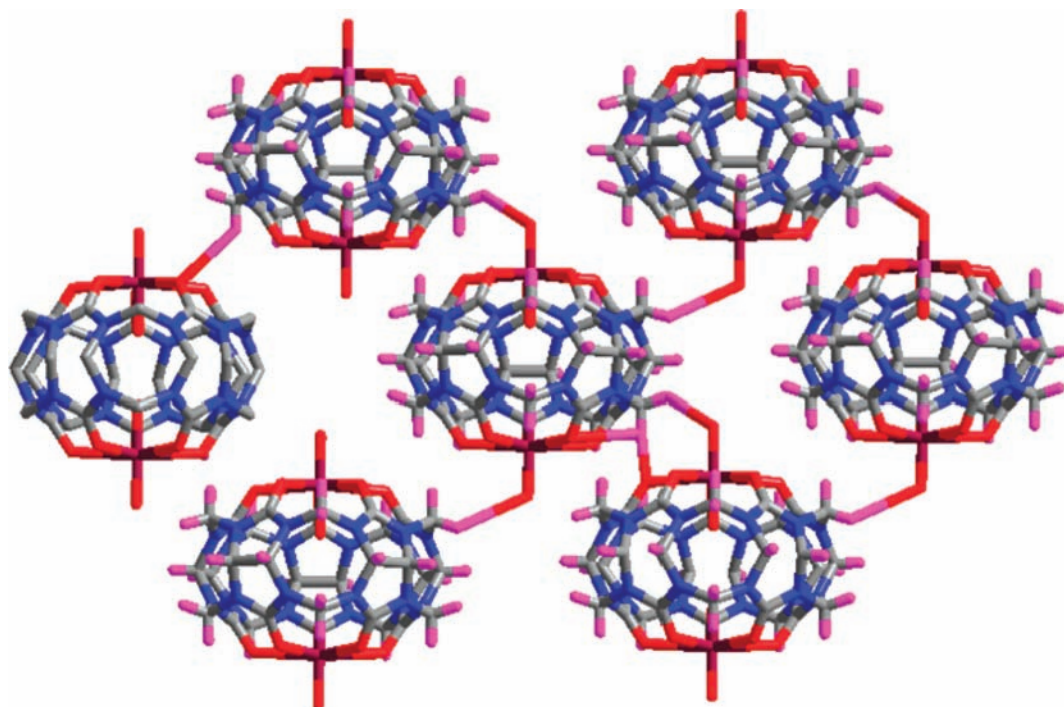


Figure 2. Environment of nitrate anion around the uranyl complex. Color code: U, heavy purple; C, gray; O, red; H, purple; N, blue.

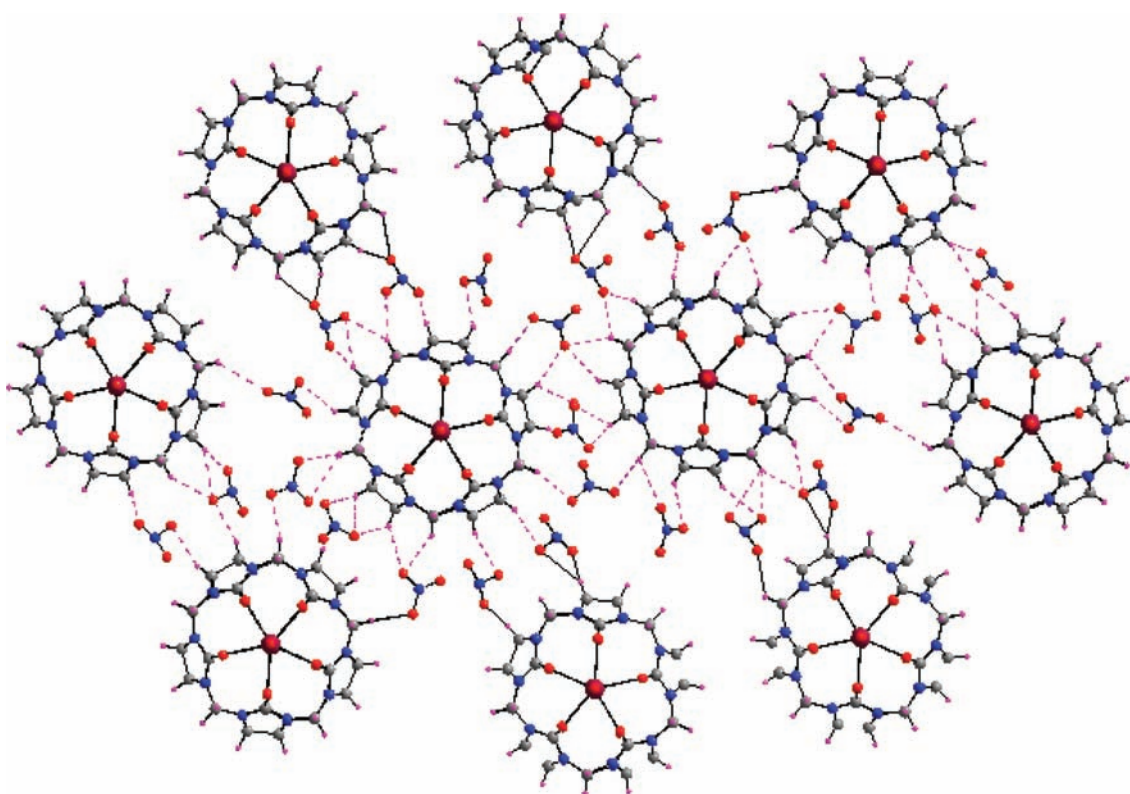


Figure 3. Two dimensional network of uranyl complex. Color code: U, heavy purple; C, gray; O, red; H, purple.

vibrations of the C–C, C–N, and C–H groups of cucurbituril were also observed. The IR spectra of the complex show strong and weak absorption bands between 950 and 850 cm^{-1} , and weak bands in the region 580 – 450 cm^{-1} (Supporting Information Figure S4). The bands at about 948 , 579 , and $\sim 480\text{ cm}^{-1}$ are assigned to the asymmetric U–O stretching modes and those at about 859 and 445 cm^{-1} to the symmetric

U–O stretching modes of the uranyl moiety.¹⁹ The strong absorption band observed at 1766 cm^{-1} may be assigned to the nitrate. Infrared spectral studies as well as X-ray structural determinations have established that in the complex, nitrate groups are acting as counterions. Stretching frequencies in the complex is significantly shifted toward lower wavenumbers (Supporting Information) Table S2 as a result of oxygen–

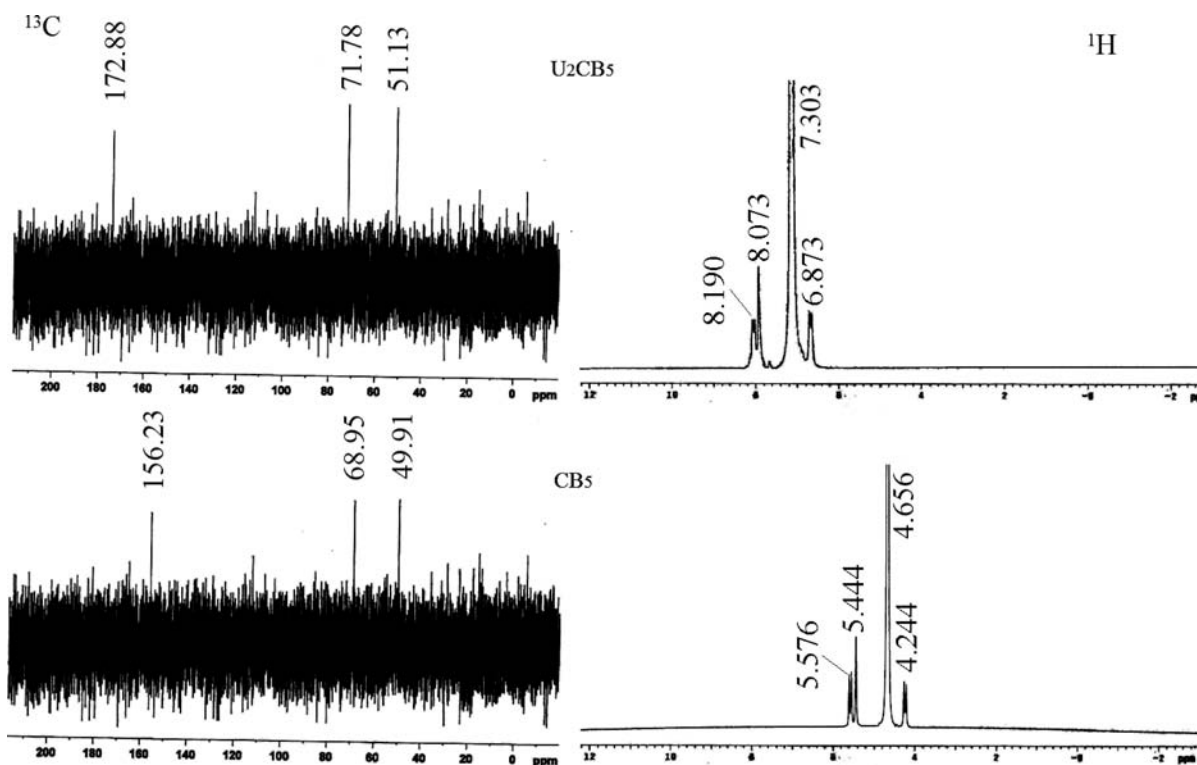


Figure 4. ^1H and ^{13}C spectra for CB5 and U2CB5.

uranium coordination. The formation of a U–O bond, leads to a decrease in the π character of the C=O bond.

Fluorescence Spectroscopy. We are also presenting here the first fluorescence study of cucurbituril complexed with uranyl ion. Uranyl nitrate was found to exhibit the typical greenish-yellow fluorescence with vibronic transitions²⁰ of uranyl ion when excited at 266 nm (Supporting Information Figure S5). The acidity of the medium seemed to play a vital role in the characteristics of the emission spectra of uranyl nitrate (Supporting Information Figure S5).²¹

Change in excitation wavelength from 266 to 330 nm to 415 nm led to an increase in resolution of the individual vibronic transitions with decrease in the intensity of emission (Figure 5 (inset)). Hence, emission for U2CB5 was measured in ~ 1.0 M HNO_3 by excitation at 266 nm at room temperature where maximum emission intensity and a well resolved spectrum was observed for uranyl nitrate at 516 nm.

The fluorescence intensity of uranyl ion increased remarkably (25.53–319), and the emission peak gradually shifted from 516 to 432 nm upon complexation with CB5 (Figure 5). The bonding of uranium to carbonyl groups and hence formation of complex with a macrocycle like CB5 suppresses the various vibrational modes present in uranyl ion.²² Furthermore the presence of two uranyl ions bound to CB5 could also be responsible for enhanced fluorescence. Thus the formation of inclusion complex of uranyl ion with CB5, led to a hypsochromic shift with fluorescence enhancement.

Increase in excitation wavelength from 266 to 330 to 415 nm led to an increase in resolution of the individual vibronic transitions while at the same time decrease in the intensity of emission was observed. The effect of acidity of the medium was also investigated by performing the experiments in 0.05, 0.10, 0.50, 1.00, 1.50, 2.0 M nitric acid. The spectra obtained by excitation at 330 nm were found to be of high emission

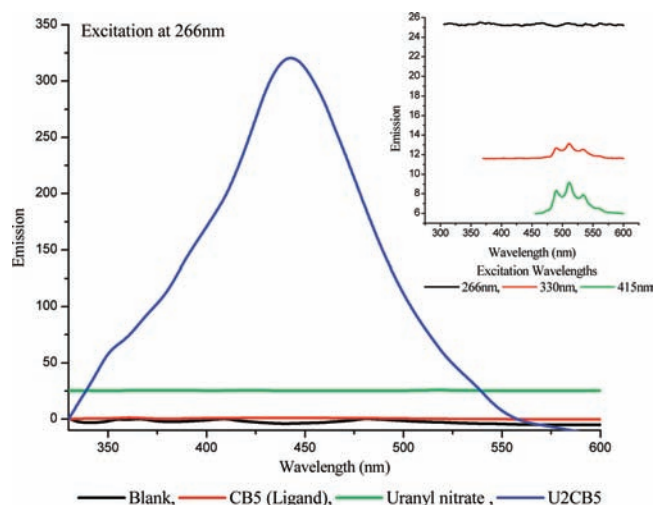


Figure 5. Emission spectra of CB5, Uranyl nitrate and U2CB5 excited at 266 nm and emission intensity measured at 432 nm. Inset: Emission intensities of uranyl nitrate excited at 266, 330, and 415 nm.

intensities and well resolved in <1 M nitric acid, while they were broad, unresolved and of lesser intensity in media containing higher concentration of nitric acid. On the other hand, the spectra obtained by excitation at 415 nm in <1 M nitric acid are found to be well resolved with maxima at 516 nm. When the concentration is increased above 1 M the peak at 518 nm is prominent with increased intensity while the other peaks appear only as shoulders. The extinction coefficient, however was much higher and the spectra were better structured for the 330 nm excitation wavelength in comparison with the 415 nm excitation wavelength. Thus the formation of inclusion complex of uranyl ion with CB5, led to a hypsochromic/blue shift with a fluorescence enhancement.

Absorption spectral characteristics of U2CB5 showed a bathochromic shift of the charge transfer band (uranium to oxygen) from 319 to 334 nm and a less intense broad shoulder in the visible region at 420 nm (Supporting Information Figure S6). The broad character of the U2CB5 could be due to electron transfer involving π -bond contribution ($d \rightarrow f$ transition).

The luminescence spectrum of a solution of uranyl nitrate (0.15 M, pH 1.3) is shown in Supporting Information Figure S5. The quantum yield of uranyl nitrate has been previously determined using fluorescein as reference, since its emission spectrum closely overlaps with that of the uranyl ion. However, fluorescein is reported to have some drawbacks as fluorescent standard because of its instability in solution and the dependence of its emission spectrum on pH.^{23a} We have, thus, determined the luminescence quantum yield for uranyl nitrate solution using, quinine sulfate in 1 M sulfuric acid (quantum yield = 0.546)^{23b} at excitation wavelength 282 nm.

Luminescence quantum yields of 2.7×10^{-3} and 0.75 were obtained for uranyl nitrate and U2CB5 respectively using quinine sulfate as standard. A quantum yield of 0.75 was also reported for the complex $[\text{UO}_2(\text{bipyO}_2)\text{H}_2\text{O}](\text{ClO}_4)_2$ by Hnatejko et al.^{23c}

CONCLUSION

In conclusion, the uranyl complex reported herein is the first molecular capsule ever reported with CB5 where both the portals are closed by uranyl ions bound to five oxygen donors obtained in a single step under ambient conditions. Another novelty is the fluorescence study of U2CB5 molecular capsule under ambient conditions which may provide new avenues for research in actinide sensing and molecular recognition and work in this direction is in progress in our laboratory.

ASSOCIATED CONTENT

Supporting Information

X-ray crystallographic data for U2CB5 in CIF format, XRPD and simulated pattern is given in Figure S1, hydrogen bonding parameters and situation are given in Figure S2, thermal analysis is provided in Table S1 and Figure S3, FTIR frequency assignments and spectra is provided in Table S2 and Figure S4, and absorption and emission spectra is given in Figure S5 and S6. This material is available free of charge via the Internet at <http://pubs.acs.org>.

AUTHOR INFORMATION

Corresponding Author

*Tel. +91-265-2795552. Fax +91-265-2795552. E-mail: p_padmaja2001@yahoo.com.

ACKNOWLEDGMENTS

Authors are thankful to Dr. Debjani Chakraborty, Dr. Sujit Baran Kumar, and Mr. Ketan Patel Department of Chemistry, The M.S. University of Baroda for their efforts in the discussions regarding crystallography.

REFERENCES

(1) Lee, J. W.; Samal, S.; Selvapalam, N.; Kim, H. J.; Kim, K. *Acc. Chem. Res.* **2003**, *36*, 621–630.
(2) Lagona, J.; Mukhopadhyay, P.; Chakrabarti, S.; Isaacs, L. *Angew. Chem., Int. Ed.* **2005**, *44*, 4844–4870.
(3) Choudhury, S. D.; Mohanty, J.; Pal, H.; Bhasikuttan, A. C. *J. Am. Chem. Soc.* **2010**, *132*, 1395–1401.

(4) (a) Kim, K. *Chem. Soc. Rev.* **2002**, *31*, 96–107. (b) Gerasko, O. A.; Samsonenko, D. G.; Fedin, V. P. *Russ. Chem. Rev.* **2002**, *71*, 741–760.
(5) Lin, J. X.; Lu, J.; Yang, H. X.; Cao, R. *Crys. Growth Des.* **2010**, *10*, 1966–1970.
(6) (a) Freeman, W. A. *Acta Crystallogr. Sect. B* **1984**, *40*, 382–387. (b) Buschmann, H. J.; Cleve, E.; Schollmeyer, E. *Inorg. Chim. Acta* **1992**, *193*, 93–97. (c) Jeon, Y. M.; Kim, J.; Whang, D.; Kim, K. *J. Am. Chem. Soc.* **1996**, *118*, 9790–9791. (d) Whang, D.; Heo, J.; Park, J. H.; Kim, K. *Angew. Chem., Int. Ed.* **1998**, *37*, 78–80. (e) Heo, J.; Kim, S. Y.; Whang, D.; Kim, K. *Angew. Chem., Int. Ed.* **1999**, *38*, 641–643. (f) Heo, J.; Kim, J.; Whang, D.; Kim, K. *Inorg. Chim. Acta* **2000**, *297*, 307–312. (g) Zhang, F.; Yajima, T.; Li, Y. Z.; Xu, G. Z.; Chen, H. L.; Liu, Q. T.; Yamauchi, O. *Angew. Chem., Int. Ed.* **2005**, *44*, 3402–3407.
(7) Liu, J. X.; Long, L. S.; Huang, R. B.; Zheng, L. S. *Cryst. Growth Des.* **2006**, *6*, 2611–2614.
(8) (a) Samsonenko, D. G.; Lipkowski, J.; Gerasko, O. A.; Virovets, A. V.; Sokolov, M. N.; Fedin, V. P.; Platas, J. G.; Hernandez-Molina, R.; Mederos, A. *Eur. J. Inorg. Chem.* **2002**, *9*, 2380–2388. (b) Samsonenko, D. G.; Gerasko, O. A.; Lipkowski, J.; Virovets, A. V.; Fedin, V. P. *Russ. Chem. Bull.* **2002**, *51*, 1915–1923. (c) Samsonenko, D. G.; Sokolov, M. N.; Gerasko, O. A.; Virovets, A. V.; Lipkowski, J.; Fenske, D.; Fedin, V. P. *Russ. Chem. Bull.* **2003**, *52*, 2132–2139. (d) Liu, J. X.; Long, L. S.; Huang, R. B.; Zheng, L. S. *Inorg. Chem.* **2007**, *46*, 10168–10173. (e) Gerasko, O. A.; Mainicheva, E. A.; Naumova, M. I.; Yurjeva, O. P.; Alberola, A.; Vicent, C.; Llusar, R.; Fedin, V. P. *Eur. J. Inorg. Chem.* **2008**, *3*, 416–424.
(9) Gerasko, O. A.; Sokolov, M. N.; Fedin, V. P. *Pure Appl. Chem.* **2004**, *76*, 1633–1646.
(10) Gerasko, O. A.; Samsonenko, D. G.; Sharonova, A. A.; Virovets, A. V.; Lipkowski, J.; Fedin, V. P. *Russ. Chem. Bull.* **2002**, *51*, 346–349.
(11) (a) Cui, S. C.; Tachikawa, T.; Fujitsuka, M.; Majima, T. *J. Phys. Chem. C* **2011**, *115*, 1824–1830. (b) Kim, K.; Selvapalam, N.; Ko, Y. H.; Park, K. M.; Kim, D.; Kim, J. *Chem. Soc. Rev.* **2007**, *36*, 267–279. (c) Burnett, C. A.; Witt, D.; Fettingner, J. C.; Isaacs, L. *J. Org. Chem.* **2003**, *68*, 6184–6191.
(12) Kim, J.; Jung, I.-S.; Kim, S.-Y.; Lee, E.; Kang, J.-K.; Sakamoto, S.; Yamaguchi, K.; Kim, K. *J. Am. Chem. Soc.* **2000**, *122*, 540–541.
(13) (a) Thuery, P. *Cryst. Growth Des.* **2009**, *9*, 1208–1215. (b) Thuery, P. *Cryst. Growth Des.* **2008**, *8*, 4132–4143. (c) Berthet, J. C.; Nierlich, M.; Ephritikhine, M. *Angew. Chem., Int. Ed.* **2003**, *42*, 1952–1954.
(14) (a) Freeman, W. A.; Mock, W. L.; Shih, N. Y. *J. Am. Chem. Soc.* **1981**, *103*, 7367–7368. (b) Kim, K.; Selvapalam, N.; Oh, D. H. *J. Inclusion Phenom.* **2004**, *50*, 31–36. (c) Otwinowski, Z.; Minor, W. *Methods Enzymol.* **1997**, *276*, 307–326. (d) Ozawa, T. C.; Kang, S. J. *J. Appl. Crystallogr.* **2004**, *37*, 679. (e) Allen, F. H. *Acta Crystallogr. Sect. B* **2002**, *58*, 380–388.
(15) (a) Wagner, B. D.; Boland, P. G.; Lagona, J.; Isaacs, L. *J. Phys. Chem. B* **2005**, *109*, 7686–7691. (b) Buschmann, H.-J.; Wolff, T. *J. Photochem. Photobiol., A* **1999**, *121*, 99–103. (c) Mohanty, J.; Nau, W. M. *Angew. Chem., Int. Ed.* **2005**, *117*, 3816–3820. (d) Saleh, N.; Al-Soud, Y. A.; Al-Kaabi, L.; Ghosh, I.; Nau, W. M. *Tetrahedron Lett.* **2011**, *52*, 5249–5254. (e) Rankin, M. A.; Wagner, B. D. *Supramol. Chem.* **2004**, *16*, 513–519. (f) Kosower, E. M. *Acc. Chem. Res.* **1982**, *15*, 259–266. (g) Saleh, N.; Al-Rawashdeh, N. A. F. *J. Fluoresc.* **2006**, *16*, 487–493. (h) Pozo, M.; Hernandez, L.; Quintana, C. *Talanta* **2010**, *81*, 1542–1546. (i) Megyesi, M.; Biczok, L.; Jablonkai, I. *J. Phys. Chem. C* **2008**, *112*, 3410–3416. (j) Yang, J. Y.; Shen, A. Z.; Du, L. M.; Li, C. F.; Wu, H.; Chang, Y. X.; Chin, J. *J. Anal. Chem.* **2010**, *38*, 1813–1816. (k) Li, C. J.; Li, J.; Jia, X. S. *Org. Biomol. Chem.* **2009**, *7*, 2699–2703. (l) Zhou, Y. Y.; Sun, J. Y.; Yu, H. P.; Wu, L.; Wang, L. *Supramol. Chem.* **2009**, *21*, 495–501. (m) Li, C. F.; Du, L. M.; Wu, W. Y.; Sheng, A. Z. *Talanta* **2010**, *80*, 1939–1944. (n) Zhou, Y. Y.; Yang, J.; Liu, M.; Wang, S. F.; Lu, Q. *J. Lumin.* **2010**, *130*, 817–820. (o) Miskolczy, Z.; Megyesi, M.; Tarkanyi, G.; Mizsei, R.; Biczok, L. *Org. Biomol. Chem.* **2011**, *9*, 1061–1070. (p) Li, C. F.; Du, L. M.; Zhang, H. M. *Spectrochim. Acta, Part A* **2010**, *75*, 912–917. (q) Occello, V. N. S.; Veglia, A. V. *Anal. Chim. Acta* **2011**, *689*, 97–102.

(16) (a) *SAINT: Software for the CCD Detector System*; Bruker Analytical X-ray Systems, Inc.: Madison, WI, 1998. (b) *Bruker SADABS, SMART, SAINTPLUS and SHELXTL*; Bruker AXS Inc.,: Madison, WI, USA, 2003. (c) Sheldrick, G. M. *SHELXS-97, Program for Structure Solution of crystal structure*; University of Göttingen: Göttingen, Germany, 1997. (d) Sheldrick, G. M. *SHELXL-97, Program for Crystal Structure Analysis*; University of Göttingen: Göttingen, Germany, 1997.

(17) (a) Cardinaels, T.; Ramaekers, J.; Guillon, D.; Donnio, B.; Binnemans, K. *J. Am. Chem. Soc.* **2005**, *127*, 17602–17603. (b) Ahmadi, S. J.; Kalkhoran, O. N.; Arania, S. S. *J. Hazard. Mater.* **2010**, *175*, 193–197.

(18) Zhang, Y.; Livens, F. R.; Collison, D.; Helliwell, M.; Heatley, F.; Powell, A. K.; Wocadlo, S.; Eccles, H. *Polyhedron* **2002**, *21*, 69–79.

(19) Hnatejko, Z.; Lis, S.; Stryła, Z.; Starynowicz, P. *Polyhedron* **2010**, *29*, 2081–2086.

(20) (a) Bartleet, J. M.; Denning, R. G.; Morrison, I. D. *Mol. Phys.* **1992**, *75*, 601–612. (b) Denning, R. G. *Struct. Bonding (Berlin)* **1992**, *79*, 215–276. (c) Liu, G.; Beitz, J. V. In *The Chemistry of the Actinide and Transactinide Elements*; Morss, L. R., Edelstein, N. M., Fuger, J., Eds.; Springer: Heidelberg, 2006; p 2088.

(21) Katsumura, Y.; Abe, H.; Yotsuyanagi, T.; Ishigure, K. *J. Photochem. Photobiol., A* **1989**, *50*, 183–197.

(22) Rabinowitch, E.; Belford, R. L. *Spectroscopy and Photochemistry of Uranyl Compounds*; Pergamon Press: Oxford, 1964; p 264.

(23) (a) Formosinho, S. J.; Miguel, M. G.; Burrows, H. D. *J. Chem. Soc., Faraday Trans.* **1984**, *80*, 1717–1733. (b) Formosinho, S. J.; Burrows, H. D.; Miguel, M. G.; Emilia, M.; Azenha, D. G.; Saraiva, I. M.; Catarina, A.; Ribeiro, D. N.; Khudyakov, I. V.; Gasanov, R. G.; Bolte, M.; Sarakha, M. *Photochem. Photobiol. Sci.* **2003**, *2*, 569–575. (c) Hnatejko, Z.; Lis, S.; Starynowicz, P.; Stryła, Z. *Polyhedron* **2011**, *30*, 880–885.